Effect of Axial Agitator Configuration (Up-Pumping, Down-Pumping, Reverse Rotation) on Flow Patterns Generated in Stirred Vessels

*J. AUBIN, P. MAVROS, D.F. FLETCHER, J. BERTRAND AND C. XUEREB**

Aubin J., Mavros P., Fletcher D.F., Xuereb C., and Bertrand J., 'Effect of Axial Agitator Configuration (Up-pumping, Down-pumping, Reverse Rotation) on Flow Patterns Generated in Stirred Vessels', *ChERD Trans IChemE*, 79, A8, 845-856, (2001).

ABSTRACT

Single phase turbulent flow in a tank stirred with two different axial impellers - a pitched blade turbine (PBT) and a Mixel TT (MTT)- has been studied using Laser Doppler Velocimetry. The effect of the agitator configuration, i.e. up-pumping, down-pumping and reverse rotation, on the turbulent flow field, as well as power, circulation and pumping numbers has been investigated. An agitation index for each configuration was also determined. In the down-pumping mode, the impellers induced one circulation loop and the upper part of the tank was poorly mixed. When up-pumping, two circulation loops are formed, the second in the upper vessel. The PBT pumping upwards was observed to have a lower flow number and to consume more power than when down-pumping, however the agitation index and circulation efficiencies were notably higher. The MTT has been shown to circulate liquid more efficiently in the up-pumping configuration than in the other two modes. Only small effects of the MTT configuration on the power number, flow number and pumping effectiveness have been observed.

Key-words: mixing, axial agitator, pitched blade turbine, Mixel TT, up-pumping, Laser Doppler Velocimetry

INTRODUCTION

Mechanically agitated vessels are widely used in the chemical, mineral and wastewater processing industries for simple fluid mixing or even complex multiphase processes including gas-liquid and gas-liquid-solid mixing. In such complex applications, the agitator has goals of circulation and homogenization, holding the gas within the vessel for as long as possible, and /or suspending solids, promoting contact between gas, liquid and solid phases. The study and understanding of the flow produced by agitators in such stirred vessels is very important as it allows the performance of an agitator to be quantified and then, if necessary, optimized in order to achieve the desired process results. In the early 1980s, it was proposed that inverting axial flow impellers and changing their rotational direction giving an 'up-pumping' effect could be interesting for gas-liquid applications[1,2]. Recently, it has been shown that up-pumping axial hydrofoil impellers provide considerable advantages over the down-pumping configuration[3-5] and this has led to the manufacture of axial hydrofoils specifically designed for up-pumping applications[6-8]. Most of the recent studies on the up-pumping concept have concentrated mainly on power characteristics and mixing times, and have shown that by applying up-pumping impellers to gas-liquid systems torque and flow instabilities are reduced, flooding is less likely to occur and there is no loss in power upon gassing[9-11].

Laser Doppler Velocimetry (LDV) is a successful experimental technique used for the study of flow fields, having the advantage of being non-intrusive. By investigating the flow patterns produced by an impeller and relating them to various global indices, such as the power number, pumping and circulation efficiencies, the performance of the mechanically agitated vessel can be quantified and optimized. With respect to the study of axial flow impellers, there have been a limited number of investigations using LDV to determine local characteristics of velocity fields and turbulence, especially when the impellers are operated in the up-pumping mode. Ranade and Joshi[12] carried out a detailed LDV study on down-pumping pitched blade turbines, investigating the influence of the impeller size and geometry on the flow patterns in the vessel. Mavros *et al.*[13] used LDV to compare the flow fields of a radial flow turbine and two different down-pumping axial flow impellers in both water and a non-Newtonian fluid. Evaluation of the performance of two commercial down-

flow impellers, the Chemineer HE3 (CHE3) and the Prochem Maxflo T (PMT), using LDV to detail the mean and r.m.s. velocities was carried out by Jaworski *et al.*[14]. A comparison of flow fields, as well as flow and circulation characteristics, produced by an APV-B2 impeller in the down- and up-pumping modes were reported by Mishra *et al.*[15]. In the down-pumping configuration, the flow fields were similar to those reported by the other workers mentioned above and it was observed that the liquid in the upper part of the vessel was poorly circulated. It was shown that by operating the impeller in the up-pumping mode, two distinct circulation loops were produced, one in the upper and one in the lower part of the vessel, and as a consequence the agitation in the upper part of the tank was improved.

In the present work, single-phase flow patterns in a stirred vessel have been investigated using LDV in a turbulent flow regime using two different axial impellers, a 6-bladed 45° pitched bladed turbine (PBT) and a Mixel TT (MTT) (Mixel, France). Comparisons have been made of the flow fields produced when the impellers are operated in the down- and up-pumping modes, and the reverse mode for the MTT. These velocity fields have been assessed by examining the power consumption, circulation and pumping capacities of the impeller, the agitation index, as well as spatial distributions of r.m.s velocities and turbulent kinetic energy. This investigation has been carried out, not only to characterize impellers operating in the up-pumping mode, being different than what has been previously published, but also to show the effects of the impeller configuration on flow fields and mixing efficiency which can easily be altered by a simple retrofitting operation. The results presented here will be used as a reference for future experimental gas-liquid mixing studies and for the validation of CFD models in stirred tanks.

EXPERIMENTAL APPARATUS AND PROCEDURES

Time-averaged LDV measurements of radial, axial and tangential velocity components were performed in a dished-bottom cylindrical vessel made of Perspex (T = 0.19 m). An aspect ratio of 1 was used, i.e. the liquid height (H) in the vessel was equal to the tank diameter (T). The tank was equipped with four transparent baffles made of Perspex ($b = T/10$), which were placed 90º from one another, flush against the vessel wall. The impeller clearance was $C = T/3$, where C is defined as the distance from the vessel bottom to the lowest horizontal plane swept by the impeller. The cylindrical vessel was placed inside a square tank, whose front panel was made of Altuglas™ to allow distortion-free measurements; this tank was filled with water in order to minimize refraction at the cylindrical surface of the inner vessel.

Two impellers were studied: a 6-blade 45° pitched blade turbine and a Mixel TT axial agitator (Mixel, France). The impeller diameter was equal to $D = T/2$ in all cases and the agitator shaft (s = 0.008 m) extended to the bottom of the vessel, where it fitted into a Teflon hub to avoid 'wobbling' of the impeller. The vessel was filled with plain tap water and was seeded using a small amount of Iriodin 111 Rutile Fine Satin (Merck) particles (d_p=15 μm). The rotational speed of the agitator, N, was 5 Hz (= 300 rpm), which corresponded to a Reynolds number of 45000. The description of the different operational modes of the impellers is as follows:

(a) Down-pumping mode: The impeller is operated in the classical manner, i.e. the impeller is rotated so that blades push the fluid downwards.

(b) Reverse mode: The rotational direction of the impeller is reversed with the impeller remaining in a downwards position.

(c) Up-pumping mode: The impeller is turned upside down and the direction of rotation is the reverse of the down-pumping mode.

The LDV measurements were taken with a two-beam Dantec Fiberflow system, operating in back-scattering mode, as shown in Figure 1. The light source is a 4 W Argon ion laser (Stabilite 2017 by Spectra Physics) with a focal length of 600 mm and beam wavelengths of 514.5 nm (green) and 488 nm (blue). The Doppler signal was transmitted to a 58N20 Flow Velocity Analyzer (Dantec) for signal processing and the results were then collected on a computer.

Measurements were taken on a plane midway between two baffles. 5000 validated samples were taken at each measuring point, with a maximum sampling time of 400 seconds. A seeding particle 'residence time' weighting was applied when calculating the mean velocity from the distribution in order to eliminate the bias towards higher values caused by high velocity particles and their consequent short residence time within the measuring volume.

The time-averaged velocity data obtained by LDV is used to determine the 2D radial-axial velocity vector fields, and flow maps of the tangential and r.m.s velocities, as well as turbulent kinetic energy. Global quantities are also calculated including the power number, the flow number and the circulation number and time, as well as performance indices such as the circulation efficiency, the pumping efficiency and the agitation index.

Power Measurements

The power consumption, P, of each agitator configuration was determined by measuring the torque using the integrated torque meter of a Labmaster mixer (Lightnin). Torque measurements were corrected for frictional losses using measurements taken in an empty vessel.

Pumping and Circulation Flow Rates

The pumping flow rate or pumping capacity, Q_{Fl}, corresponds to the fluid flow rate that passes through the impeller swept volume[16]. For reasons of practicality, this calculation is performed on a control volume, which just encompasses the impeller swept volume, as shown by relation (1):

$$Q_{Fl} = \int_{z^{--}}^{z^{++}} \pi D \left| \left(v_r^o \right)_{r=r^{++}} \right| dz + \int_{0}^{r^{++}} 2\pi r \left| \left(v_z^o \right)_{z=z^{++}} \right| dr + \int_{0}^{r^{++}} 2\pi r \left| \left(v_z^o \right)_{z=z^{--}} \right| dr \qquad (1)$$

where z^{++}, z^{--} and r^{++} are the boundaries of the impeller control volume and the superscript 'o' refers to the fluid moving *out* of this volume. This expression takes into account both radial and axial pumping flow rates.

The discharge flow rate of the impeller may then be expressed as the dimensionless pumping number by normalizing Q_{Fl} by ND^3:

$$Fl = \frac{Q_{Fl}}{ND^3} \qquad (2)$$

The circulation flow rate, Q_c, in the tank is the total volumetric turnover rate occurring in the tank. It is the sum of the discharged fluid flow and the flow entrained by the impeller[16]. Assuming axial symmetry, the

absolute maximum values of the axial flow rate, Q_z, in the vessel is equal to the total circulation flow rate[14]. This circulation flow rate may be evaluated by calculating the flow rate through a plane that passes through the centre of the circulation loop with radial-axial coordinates (r^*, z^*)[17].

$$Q_z = Q_c = \int_{r^*}^{R} 2\pi r \left| \left(v_z\right)_{z=z^*} \right| dr \tag{3}$$

where r^* and z^* are the coordinates of the loop centre. In the presence of two circulation loops, the axial circulation flow rate can be given by the sum of the flow rate entrained by the lower loop and that entrained by the upper loop such that :

$$Q_c = Q_{c1} + Q_{c2} \tag{4}$$

where

$$Q_{c1} = \int_{r^*}^{R} 2\pi r \left| \left(v_z\right)_{z=z^{*1}} \right| dr \tag{5}$$

$$Q_{c2} = \int_{r^*}^{R} 2\pi r \left| \left(v_z\right)_{z=z^{*2}} \right| dr \tag{6}$$

where the superfixes 1 and 2 differentiate the lower circulation loop and the upper circulation loop.

Normalizing the circulation flow rate by ND^3, results in the dimensionless circulation flow rate number, Fl_c:

$$Fl_c = \frac{Q_c}{ND^3} \tag{7}$$

Using Fl, Fl_c and Po, two indices characterizing the effectiveness of an agitator can be described. The pumping effectiveness, η_E, gives the pumping rate of the impeller per unit power consumption and is given by relation (8):

$$\eta_E = \frac{Fl}{Po} \tag{8}$$

The second index is the circulation efficiency number, E_c, which indicates the impellers capacity to circulate the liquid with respect to its power consumption. This relationship, defined by Jaworski *et al.*[14] enables different types and sizes of agitators to be compared in a turbulent flow regime, independent of impeller speed.

$$E_c = \frac{Fl_c}{Po}\left(\frac{D}{T}\right)^4 \tag{9}$$

Turbulent Kinetic Energy

Accurate estimation of the turbulent kinetic energy, k_T, induced in a stirred tank requires the root mean square velocities (velocity fluctuations) of the three velocity components:

$$k_T = \frac{1}{2}\left(\left\langle v_r'^2 \right\rangle + \left\langle v_z'^2 \right\rangle + \left\langle v_\theta'^2 \right\rangle\right) \tag{10}$$

This quantity is made dimensionless by dividing by the square of the impeller tip speed, V_{tip}^2.

Agitation Index

Mavros and Baudou[18] defined an agitation index, I_g, in order to determine the effectiveness of an impeller to induce flow in a tank. I_g is calculated with the resultant mean velocity, v_{ij}, of the three time-averaged velocity components at each measuring point in the vessel. It is supposed that the each resultant velocity corresponds to a liquid volume V_{ij}, surrounding the measuring point. The liquid volumes in the vessel are summed and a volume weighted average velocity for the entire tank is obtained:

$$\hat{v} = \frac{\sum_i \sum_j \mathrm{v}_{ij} V_{ij}}{\sum_i \sum_j \mathrm{V}_{ij}} \tag{11}$$

The volume-weighted velocity is then normalized by V_{tip} to give the agitation index, I_g:

$$I_g = 100\frac{\hat{v}}{V_{tip}}[\%] \tag{12}$$

For further details on the definition and calculation of the agitation index, readers are referred to Mavros and Baudou[18].

RESULTS AND DISCUSSION

Mean Velocity Fields and Flow Patterns

Down-Pumping

Vector plots of time-averaged velocity fields in the r-z plane at 45° to the baffle plane for the PBTD and the MTTD are shown in Figures 2(a) and 2(b). These plots show that a circulation loop is formed in the lower part of the vessel; in the upper part of the tank, liquid velocities are low, circulation is minimal and therefore mixing is rather poor. These observations are characteristic of down-pumping axial agitators. In the outflow of the impeller, the fluid is discharged axially for the most part – for the PBTD, a noticeable radial component exists in this region which confirms the observations made be Ranade and Joshi[12]. Once the down-flowing high speed jet encounters the vessel bottom, the fluid moves along the bottom and then up the vessel wall. Due to low pressure regions behind the impeller blades, most of the fluid is taken in at the top of the impeller-swept volume, with some being drawn into the side. This causes the formation of a primary circulation loop. Little liquid movement is observed in the upper part of the vessel for both impellers, although circulation for the PBTD-stirred tank appears to be more significant. A third fluid zone exists in the vessel stirred by the PBTD, which is a conical

region of up-flowing liquid below the centre of the impeller. This observation has already been made for pitched-blade turbines and also other axial impellers, including the Chemineer HE3 (CHE3), the Prochem Maxflo T (PMT) and the APV-B2[12, 14, 15].

Considering the axial velocity component for both impellers, the maximum down-flowing velocities occur in the impeller discharge region and the maximum positive values of axial velocities are found close to the vessel wall. The axial down-flow induced by the PBTD is approximately 10% greater than that induced by the MTTD being 44% and 39% of V_{tip} respectively. For both agitators, the maximum up-flowing velocity is approximately 22% less than the discharge flow at 36% and 30% of V_{tip} for the PBTD and MTTD. In the upper part of the tank, axial velocities are small, with a value of about 2% of V_{tip}, flowing generally downwards. Such low velocities in this region of the tank indicate quantitatively poor circulation and mixing. The cone-shaped up-flow zone observed in the tank agitated by the PBTD has a maximum velocity of 7% of V_{tip}. This result compares well with the work of Ranade and Joshi[12], who found a maximum velocity of 5% of V_{tip} in this region for a PBTD.

The radial velocity component is high in the planes above and below the impeller. The liquid being drawn in by the impeller (with a maximum radial velocity) is at 14% V_{tip} for the PBTD which is slightly lower than 15% V_{tip} for the MTTD. However, the liquid discharged below the PBTD has a greater maximum velocity, 22% of V_{tip}, than the MTTD at 15% V_{tip}. Similar maximal discharge velocities have already been reported for a PBTD (25% V_{tip})[12], a PMT and a CHE3 (22% and 20% of V_{tip}, respectively)[14].

Contour maps for the tangential velocity component are presented in Figure 3. For both impellers, maximum tangential velocities are very localized and in the rest of the vessel only small tangential velocities exist. The PBTD induces a maximum tangential velocity at the tip of the impeller which is 63% of V_{tip} and the MTTD produces the maximal tangential velocity below the centre of the agitator with a significantly lower value of 32% V_{tip}. The latter is evidence of a small region of swirling liquid with minimal radial /axial movement. In the upper part of the tank, a small zone of liquid close to the vessel wall is observed to rotate in the opposite direction to the agitator rotation. Although this effect is slight (~1.7% % of V_{tip} for both the PBTD and the MTTD), it has already been reported by Mavros *et al.*[13].

Up-pumping

Velocity vectors in the *r-z* plane for the impellers in the up-pumping configuration are shown in Figure 2. Operation of the impellers in this mode induces two circulation loops, one in the upper part of the tank and one in the lower part. These observations confirm previous works on up-pumping hydrofoil impellers and pitched blade turbines[15, 19]. The agitator generates a strong discharge flow into the upper part of the vessel that is projected at approximately 45° towards the vessel wall. Due to this strong radial component, the liquid is propelled towards the vessel wall where it either moves axially up to the liquid surface or down to the tank bottom. In the lower half of the tank, the liquid is forced down the vessel wall and upon encountering the tank base, its movement is redirected in an upwards direction and is drawn into the underside of the impeller swept region. This circulation path forms the primary circulation loop.

For the MTTU, liquid is drawn in by the underside of the impeller as well as at the vertical side of the impeller. Axial movement of the liquid close to the vessel in the upper region of the tank experiences a change in direction due to the liquid surface. This gives rise to the secondary circulation loop with an ensuing downward

flow and induces fluid velocities in the upper region of the tank higher than those observed in the down-pumping mode, and therefore the degree of circulation and mixing appears to be better. A third observation has been made for the flow produced by the PBTU – a region of down-flowing liquid into the centre of the upper side of the impeller exists, as seen also in the down-pumping configuration. Mishra *et al.*[15] have reported similar flow patterns for an up-pumping APV-B2 including the presence of two distinct circulation loops, as well as a small down flowing region in the centre of the upper side of the impeller. It should be noted that the velocities induced by the PBTU in the upper region of the vessel and at the bottom vessel corners appear greater than in the case of the MTTU, indicating a stronger overall circulation for the PBTU.

For the two impellers, a strong axial flow of liquid moving upwards, into and out of the impeller-swept volume is observed. High axial velocities are also noticed to be moving down the vessel wall in the lower half of the tank. The fluid in the vessel agitated by the PBTU also exhibits high up-flowing velocities close to the vessel wall in the upper part of the vessel, which are not observed with the MTTU. The PBTU induces considerably higher axial velocities than the MTTU – maximums of 41% V_{tip} compared with 28% V_{tip} for up-flowing velocities and 51% V_{tip} compared with 31% V_{tip} in the downwards direction. It is also observed that the downward flowing velocities are stronger than those moving upwards in the case of both agitators. For the PBTU, this effect is relatively important, as the maximum down-flowing axial velocity is ~25% greater than the maximum velocity flow upwards.

For both up-pumping impellers, an important out-flowing radial movement is observed above the impeller in the discharge zone, as well as two zones of high inward-flowing velocities, which are situated close to the tank bottom and near the free liquid surface. In the impeller discharge, the maximum velocity for the PBTU is at 37% of V_{tip} and for the MTTU it is at 23% of V_{tip}. Mishra *et al.*[15] reported a maximum radial velocity in the discharge region of the APV-B2 agitator of 33% of V_{tip}. The zones of highest in-flowing velocity are found in the lower part of the vessel, the PBTU induces a maximum radial velocity of 23% of V_{tip}, whereas for the MTTU this value is 15% of V_{tip}. These velocities below the impeller are greater than the ones found for the APV-B2, which were reported to be less than 10% V_{tip}[15]. In the upper vessel, these radial velocities are high, but lower than those observed below the impeller, especially for the MTTU.

The maximum tangential velocity distributions in the up-pumping impeller configurations – Figures 3(c) and 3(d) – differ considerably from those of the down-pumping configurations. Here, the maximum velocities are, for the most part, localized in the impeller discharge, and in the case of the PBTU a strong tangential flow is also observed below the centre of the agitator. It should be noted, however, that these velocity magnitudes are substantially lower for the up-pumping configuration, being 22% and 18% of V_{tip} for the PBTU and MTTU respectively, when compared with the values measured for the down-pumping arrangement. Close to the impeller shaft (in the upper part of the vessel for the PBTU and in the lower part for the MTTU) the liquid moves in the direction of rotation at ~ 10% of V_{tip}. Like for the down-pumping mode, liquid is observed to rotate in the reverse direction in the upper part of the vessel and also below the MTTU. For the PBTU, this reverse rotation effect is of a similar magnitude to the down-pumping configuration (1.5% of V_{tip}). For the MTTU however, the maximum reverse velocity is found to be 4.1% of V_{tip} in both the upper and lower regions of the tank.

Reverse Mode

The r-z plane vector plots are shown in Figure 2. The flow pattern observed for the MTTR is similar to that produced by the MTTU. Two circulation loops are formed in the vessel, the primary in the lower half of the tank and the secondary in the upper part. As the impeller discharge is not as strong as in the up-pumping mode, the upper circulation loop is slightly less significant.

Both the axial and radial flow patterns are very similar to those induced by the MTTU. Axially, the maximum velocities occur below the impeller where the liquid is drawn and in the discharge above the impeller (22% of V_{tip}), as well as maximum down-flowing velocities close to the vessel wall in lower half of the tank (24% of V_{tip}). These values are approximately 20% lower than those induced by the MTTU. Concerning the radial velocity component, three high velocity zones are observed as previously noted for the up-pumping configurations. The MTTR produces maximum radial velocities above and below the impeller with a zone of relatively high velocity close to the liquid surface. For in-flowing (negative) radial velocities, the maximum is 15% of V_{tip} which is not much different to that found for the MTTU. The out-flowing radial velocities for the MTTR are however smaller (16% of V_{tip}) in comparison with those of the MTTU (23% of V_{tip}). The tangential The tangential velocity map is shown in Figure 3(e). Maximum tangential flow is observed at the impeller tip and in the centre below the impeller with a value of 15% V_{tip}. Again, liquid rotating in the counter direction is observed in the upper part of the vessel reaching a maximum of 3.2% V_{tip}.

R.m.s. Velocities and Turbulent Kinetic Energy

Figures 4-6 show contour maps of the r.m.s. velocities for each of the velocity components in the down, up and reverse modes. In all three pumping configurations, the r.m.s. velocities are considerably higher in the discharge stream of the impeller than in the bulk of the tank. In the up-pumping and reverse modes, the high r.m.s. velocity region around the impeller is more spread out than in the down-pumping mode. Even though the r.m.s. velocities observed in the bulk of the tank are significantly smaller than the maximums found in the discharge flow, the difference between the component values varies noticeably. Table 1 gives the maximum r.m.s values for each impeller configuration. From these results, it is reserved that the flow induced by these two impellers in the three different configurations is in general, not isotropic. Mishra *et al.*[15] have also observed that the flows induced by an APV-B2 impeller in both the up- and down-pumping configurations are not isotropic.

Figure 7 presents spatial distributions of dimensionless turbulent kinetic energy ($k^* = k_T/V^2_{tip}$), determined using the three r.m.s. components. For the three pumping configurations, the maximum values of k^* are generally found in the impeller discharge region. For the PBTD, the highest k^* values are found at the impeller tip and just below with a maximum of 14% of V^2_{tip}. This value is somewhat higher than 9% of V^2_{tip} for a 6-bladed pitched blade turbine ($D = T/3$)[20]. The spatial distribution of k^* for the MTTD is similar to that reported by Mavros *et al.* (1998) and its maximum value of 3.4% V^2_{tip} is comparable with 3.2% of V^2_{tip} for a $T/3$ propeller[20] and 2.7% of V^2_{tip} for an down-pumping APV-B2[15]. In the up-pumping and reverse modes, the maximum turbulent kinetic energy values are smaller than for the down-pumping configuration, although the high energy regions are larger in size. The largest difference is for the PBTU with a maximum value of only 5.0% V^2_{tip}, for the MTTU and the MTTR the highest values are only slightly less than that found in the down-pumping mode being 2.7% and 2.5% of V^2_{tip}, respectively.

Power, Pumping and Circulation

Power and flow characteristics of the different impellers and configurations are presented in Table 2. In the down-pumping mode, the PBTD exhibits a power number which is in the same range as previously reported values[12, 20, 22, 23] and is approximately 2.5 times greater than that of the MTTD. The value for this latter impeller is comparable with other studies of the MTTD[13, 24]. In the up-pumping mode, the power number for the PBTU is 33% greater than in the down-pumping configuration. Not such a great difference is shown for the power numbers of the down-, up-pumping and reverse modes for the MTT. When up-pumping and in reverse rotation, power consumption decreases only slightly in a progressive manner. The flow numbers for both impellers in the up-pumping mode are slightly inferior to those for the down-pumping mode which is in good agreement with flow number data found for a down- and up-pumping APV-B2[15]. The flow number for the MTTR however is approximately 33% smaller than the down- and up- pumping modes.

Assessment of the circulation numbers shows that in the up-pumping configuration, circulation is much greater than in the down-pumping mode. This is with a consequence of the second circulation loop formed in the upper part of the vessel when the agitator pumps upwards. Circulation produced by the MTTR is poorer than both the down- and up- pumping configurations. The pumping effectiveness for the three configurations of the MTT is greater than both pumping modes of the PBT. The PBTD uses power more effectively than the PBTU, although there is no difference between the down- and up-pumping modes of the MTT. As expected, the pumping effectiveness of the MTTR is less than in the other configurations. The last index shows clearly that the up-pumping impellers circulate liquid more efficiently in the vessel. The comparatively low circulation efficiencies for the down-pumping mode reflect the poor agitation in the upper tank as already shown by the LDV data.

Agitation Index

The agitation indices, I_g, for all impeller configurations have been calculated and the results are shown in Table 3. Considering the down-pumping configurations, the global mean velocity produced by the PBTD is 16.0% of V_{tip} which is greater than the index calculated for the MTTD of 14.1%. Comparing these results with those of the up-pumping mode shows some differences. For the PBTU the agitation index is increased notably to 22.5% of V_{tip}. This is coherent with observations made from analysis of the LDV velocity data: the PBT in the up-pumping configuration induces the development of a relatively strong secondary circulation loop in the upper part of the vessel which increases the overall liquid velocity. The agitation index of the MTTU, however, is more or less the same as the down-pumping mode, even slightly inferior at 13.7%. This suggests that although the MTTU may appear to circulate liquid better than the MTTD from the vector diagrams, the agitation index shows that the global liquid velocity of the MTTU is slightly less.

In the reverse mode, the MTT is even less effective than the MTTU, giving an agitation index of only 11.9%. Mavros and Baudou[18] have presented similar results for a Rushton turbine, a down-pumping MTT and a down-pumping A310. Their agitation index for the Rushton turbine is 17.8%, which is slightly greater than the PBTD value found in this work but considerably inferior to the value found for the PBTU. This indicates a potential effectiveness for some impellers to operate in the up-pumping mode.

The distributions of liquid volumes, which are associated with a particular velocity range, have been determined for each agitator configuration and are presented using histograms in Figure 8. For the down-

pumping configurations, the liquid volume distribution is centred around a very low velocity range – 70% of the liquid volume has a velocity of less than 20% of V_{tip}. In the up-pumping mode, the distributions still have a similar form to the down-pumping distributions though their centres are shifted to higher velocity ranges, the PBTU having a more important shift than the MTTU. In the PBTU configuration, only 45% of the liquid volume has a velocity of less than 20% V_{tip}, whereas for the MTTU 60% of the liquid is moving at less than 20% V_{tip}. The reverse mode produces an uneven distribution of the liquid volumes and approximately 95% of the liquid volume has velocity of less than 25% of V_{tip}.

CONCLUSION

LDV measurements have been carried out in a vessel stirred by two different axial impellers operating in either the down-, up-pumping or reverse modes. 2-D r-z velocity vector fields and tangential velocity component maps demonstrate the differences in flow fields produced by these impellers in different operating modes. In the down-pumping mode, one circulation loop is produced and the velocities in the upper part of the tank are very weak, resulting in poor mixing. The impellers pumping upwards induce two circulation loops, one in the lower and one in the upper part of the tank. This results in a better circulation in the upper part of the vessel.

Operating in the reverse mode, the impeller produces a flow pattern similar to that of the up-pumping configuration with two circulation loops, however the velocities are much smaller. R.m.s velocities have found to be considerably higher in the impeller discharge stream than in the bulk of the tank for the three configurations and the flow is generally non-isotropic which is in agreement with previous up- and down-pumping mixing studies[15]. The maximum values of the turbulent kinetic energy are found in the impeller discharge region for the different pumping modes. The values in the up-pumping and reverse modes are however slightly smaller than for the down-pumping agitator.

Comparing pumping effectiveness of up- and down-pumping configurations reveals that the PBTU is less effective than in the down-pumping mode, although the MTTD and MTTU are equivalent. The circulation efficiency has been shown clearly to be superior for up-pumping impellers (especially for the PBT) than for the down-pumping or reverse mode operations.

In conclusion, it has been shown that by simply changing the pumping direction of axial impellers to operate in the up-pumping mode, some interesting flow features are produced. Even though power consumption and pumping effectiveness may appear to be less favourable for some up-pumping impellers in single-phase systems, circulation is considerably improved and the formation of two circulation loops may be promising for gas-liquid dispersions[10,25]. The liquid flow would interfere with the flow of the bubbles, hence retaining more gas within the vessel. This would result in higher gas holdup and interfacial areas which would possibly have positive effects on gas-liquid reactions and other gas-liquid or gas-liquid-solid contacting processes.

NOTATION

b	baffle width (m)
C	impeller clearance (m)
d_p	seeding particle diameter (μm)
D	impeller diameter (m)
D_{sh}	shaft diameter (m)

E_c	circulation efficiency (-)
Fl	flow number (-)
Fl_c	circulation number (-)
H	liquid height in tank (m)
η_E	pumping effectiveness (-)
I_g	agitation index (dimensionless)
k_T	turbulent kinetic energy (m^2s^{-1})
k^*	dimensionless kinetic energy (-)
N	impeller rotational speed (s^{-1})
P	power (W)
Po	power number (-)
Q_c	circulation flow rate (m^3s^{-1})
Q_{Fl}	pumping flow rate (m^3s^{-1})
Q_r, Q_z	radial and axial flow rates (m^3s^{-1})
r	position in the radial direction
r^*	radial coordinate of circulation loop center
r.m.s.	root mean square
R	radius of tank (m)
T	tank diameter (m)
Tu	turbulence intensity (-)
V_{ij}	liquid volume surrounding measuring point (m^3)
v_r, v_z, v_θ	velocity components (ms^{-1})
v_r', v_z', v_θ'	r.m.s. velocity components (ms^{-1})
$\hat{v}$	volume weighted average velocity (ms^{-1})
V_{tip}	impeller tip speed (ms^{-1})
z	position in the axial direction
z^*	axial coordinate of circulation loop center
$\langle\ \rangle$	time-averaged

Impeller types

CHE3	Chemineer HE3 impeller
MTTD, U, R	Mixel TT impeller, down-pumping, up-pumping, reverse rotation
PBTD, U	pitched blade turbine, down-pumping, up-pumping
PMT	Prochem Maxflo T impeller

REFERENCES

1. Kuboi R. and Nienow A.W., 1982, 'The Power Drawn by Dual Impeller Systems Under Gassed and Ungassed Conditions', Paper G2, *4th European Conference on Mixing*, Leeuwenhorst, BHRA Fluid Engineering U.K., 247-261.

2. Nienow A.W., Kuboi R., Chapman C.M. and Allsford K., 1983, 'The Dispersion of Gases into Liquids by Mixed Flow Impellers', Paper K1, *International Conference on the Physical Modelling of Multi-Phase Flow*, Coventry, BHRA Fluid Engineering U.K., 417-437.
3. Nienow A.W., 1990a, 'Gas Dispersion Performance in Fermenter Operation', *Chem. Eng. Prog.*, **85**, 2, 61-71.
4. Nienow A.W., 1990b, 'Agitators for mycelial fermentations', *TIBTECH*, **8**, 224-233.
5. Nienow A.W., 1996, 'Gas-Liquid Mixing Studies : A Comparison of Rushton Turbines with Some Modern Impellers', *Trans IChemE*, **74** A, 417-423.
6. Ozcan-Taskin N.G., Badham R.S., Dyster K.N., Jaworski Z., Moore I.P.T., Nienow A.W., Wyszynski M. and McKemmie J., 1995; 'Development and Characterisation of a New Impeller', *The 1995 IChemE Research Event*, Edinburgh, IChemE Rugby, U.K., 671-673.
7. Ozcan-Taskin N.G., Badham R.S., Dyster K.N., Jaworski Z., Moore I.P.T., Nienow A.W., Wyszynski M. and McKemmie J., 1996, 'Gas-Dispersion Performance of a Newly Designed Impeller in the Transitional Flow Regime', *The 1996 IChemE Research Event /2nd European Conference For Young Researchers*, Leeds, U.K., 112-114.
8. Kaufman P., Post T.A. and Preston M., 1998, 'Up-pumping Mixing Technology. Breaking the Mold of Traditional Systems', *Chem. Proc.*, **61**, 10, 63-66.
9. McFarlane C.M., 1991, *Gas-Liquid Mixing Studies on Hydrofoil Impellers*, PhD Thesis, The University of Birmingham, U.K.
10. Hari-Prajitno D., Mishra V.P, Takenaka K., Buljalski W., Nienow A.W. and McKemmie J., 1998, 'Gas-Liquid Mixing Studies with Multiple Up- and Down-Pumping Hydrofoil Impellers : Power Characteristcs and Mixing Time', *Can. J. Chem. Eng.*, **76**, 1056-1068.
11. Hari-Prajitno D., 1999, *An Experimental Study of Unaerated and Aerated Single, Dual and Triple Hydrofoil Impellers*, PhD Thesis, The University of Birmingham, U.K.
12. Ranade V.V. and Joshi J.B., 1989, 'Flow Generated by Pitched Blade Turbines I : Measurements Using Laser Doppler Anemometer', *Chem. Eng. Comm.*, **81**, 197-224.
13. Mavros P., Xuereb C., and Bertrand J., 1996, 'Determination of 3-D Flow Fields in Agitated Vessels by Laser Doppler Velocimetry : Effect of Impeller Type and Liquid Viscosity on Liquid Flow Patterns', *Trans IChemE*, **74** A, 658-668.
14. Jaworski Z., Nienow A.W. and Dyster K.N., 1996, 'An LDA Study of the Turbulent Flow Field in a Baffled Vessel Agitated by an Axial, Down-pumping Hydrofoil Impeller', *Can. J. Chem. Eng.*, **74**, 3-15.
15. Mishra V.P., Dyster K.N., Jaworski Z., Nienow A.W., and McKemmie J.,1998, 'A Study of an Up- and a Down-Pumping Wide Blade Hydrofoil Impeller : Part I. LDA Measurements', *Can. J. Chem. Eng.*, **76**, 577-588.
16. Tatterson G.B., 1991, 'Circulation Times and Pumping Capacities', *Fluid Mixing and Gas Dispersion in Agitated Tanks*, McGraw-Hill Inc., New York, 208-222.
17. Costes J., 1986, *Structure des Ecoulements Générés par une Turbine de Rushton dans une Cuve Chicanée*, PhD Thesis, INP, Toulouse, France.
18. Mavros P. and Baudou C., 1997, 'Quantification of the Performance of Agitators in Stirred Vessels : Definition and Use of an Agitation Index', *Trans IChemE*, **75** A, 737-745.

19. Meyers K.J. and Bakker A., 1998, 'Solids Suspension with Up-Pumping Pitched-Blade and High-Efficiency Impellers', *Can. J. Chem. Eng.*, **76**, 3, 433-440.
20. Mishra V.P., 1993, *Fluid Mechanics of Mechanically Agitated Reactors*, Ph.D. Thesis, University of Bombay, Bombay, India.
21. Mavros P., Xuereb C. and Bertrand J., 1998, 'Determination of 3-D Flow Fields in Agitated Vessels by Laser Doppler Velocimetry : Use and Interpretation of RMS Velocities', *Trans IChemE*, **76** A, 223-233.
22. Jaworski Z., Nienow A.W., Koutsakos E., Dyster K. and Bujalski W., 1991, 'An LDA Study of Turbulent Flow im a Baffled Vessel Agitated by a Pitched Blade Turbine, *Trans IChemE*, **69** A, 313-320.
23. Bakker A., 1992, *Hydrodynamics of Stirred Gas-Liquid Dispersions*, Ph.D. Thesis, Delft University of Technology, The Netherlands.
24. Baudou C., 1997, *Agitation par des Systèmes Axiaux Simples ou Multi-Etages. Obtention de l'Hydrodynamique par Vélocimétrie Laser à Effet Doppler*, Ph.D. Thesis, INP Toulouse, France.
25. Nienow A.W., 1999, 'The Versatility of Up-Pumping, Wide-Blade Hydrofoil Impellers', *Proceedings of the 3rd International Symposium on Mixing in Industrial Processes*, 173-180.

Table 1. Maximum r.m.s values.

Impeller	V_z'/V_{tip}	V_r'/V_{tip}	V_θ'/V_{tip}
PBTD	0.20	0.24	0.5
PBTU	0.18	0.21	0.28
MTTD	0.19	0.15	0.16
MTTU	0.15	0.16	0.12
MTTR	0.11	0.14	0.12

Table 2. Power and flow characteristics of the impellers used in this work.

Impeller	*Po*	*Fl*	Fl_c	η_E	E_c
PBTD	2.21[a], 2.1[b], 1.70[c], 1.55[d], **1.93**[g]	0.8[a], 0.91[b], 0.73[c], 0.81[d], **0.75**[g]	1.73[b], 1.38[c], **0.91**[g]	0.43[b], **0.39**[g]	0.029[b], **0.024**[g]
PBTU	**2.58**[g]	**0.68**[g]	**1.82**[g]	**0.26**[g]	**0.146**[g]
MTTD	0.65[e], 0.60[f], **0.74**[g]	0.73[e], 0.63[f], **0.67**[g]	0.91[e], 0.79[f], **1.13**[g]	1.12[e], 1.05[f], **0.91**[g]	**0.122**[g]
MTTU	**0.67**[g]	**0.61**[g]	**1.35**[g]	**0.91**[g]	**0.230**[g]
MTTR	**0.62**[g]	**0.44**[g]	**1.08**[g]	**0.71**[g]	**0.127**[g]

[a] Ranade and Joshi[12]; [b] Mishra[20]; [c] Jaworski *et al.*[22]; [d] Bakker[23]; [e] Mavros *et al.*[13]; [f] Baudou[24]; [g] This work.

Table 3. Agitation index for the various impellers used in the present work.

	Pumping mode		
Impeller	**Down**	**Up**	**Reverse**
PBT	16.0%	22.5%	-
MTT	14.1%	13.7%	11.9%

Figure 1. Experimental set-up : (1) Laser source, (2,3) Fiber-optical module, (4) Photomultipliers, (5) Flow velocity analyser, (6) Oscilloscope, (7) Computer.

Figure 2. 2D flow maps of axial-flow impellers: (a) PBTD; (b) MTTD; (c) PBTU; (d) MTTU; (e) MTTR.

Figure 3. 2D flow maps of the dimensionless tangential velocity component, V_θ/V_{tip} : (a) PBTD; (b) MTTD; (c) PBTU; (d) MTTU; (e) MTTR.

Figure 4. RMS velocity distribution maps for the downwards-pumping impellers: (a) PBTD; (b) MTTD.

Figure 5. RMS velocity distribution maps for the upwards-pumping impellers: (a) PBTU; (b) MTTU.

Figure 6. RMS velocity distribution maps for the reverse-rotating MTT impeller.

Figure 7. Maps of dimensionless turbulent kinetic energy, $k^* = k_T/V^2_{\text{tip}}$.

Figure 8. Distribution of liquid volume fractions in the vessel with respect to dimensionless composite velocity intervals.

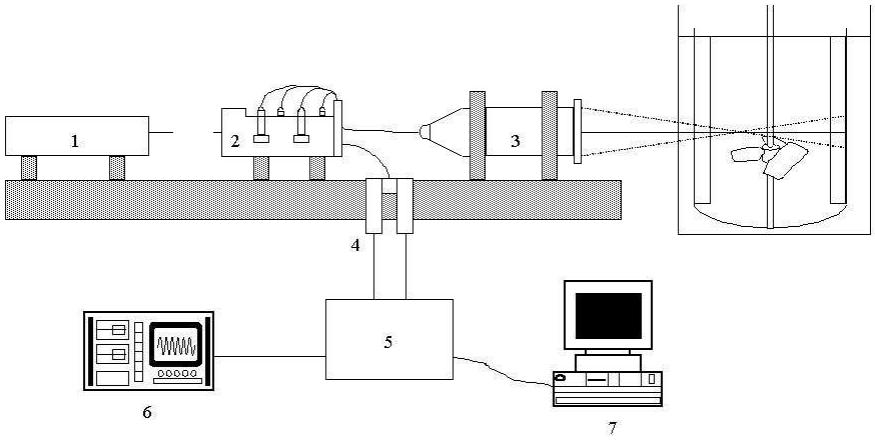

Figure 1

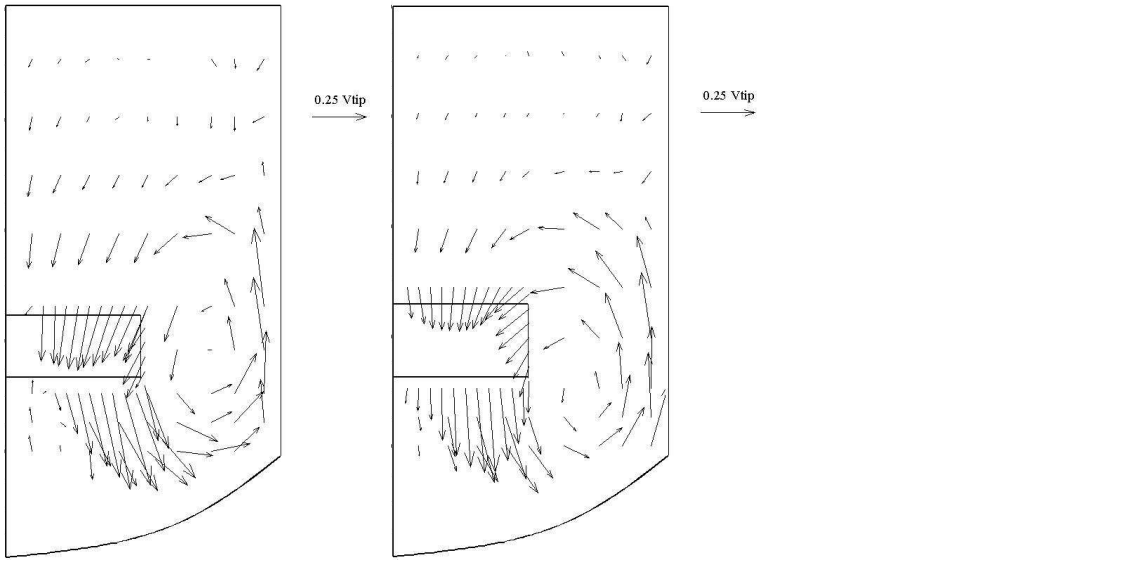

(a) PBT-downwards (b) MTT-downwards

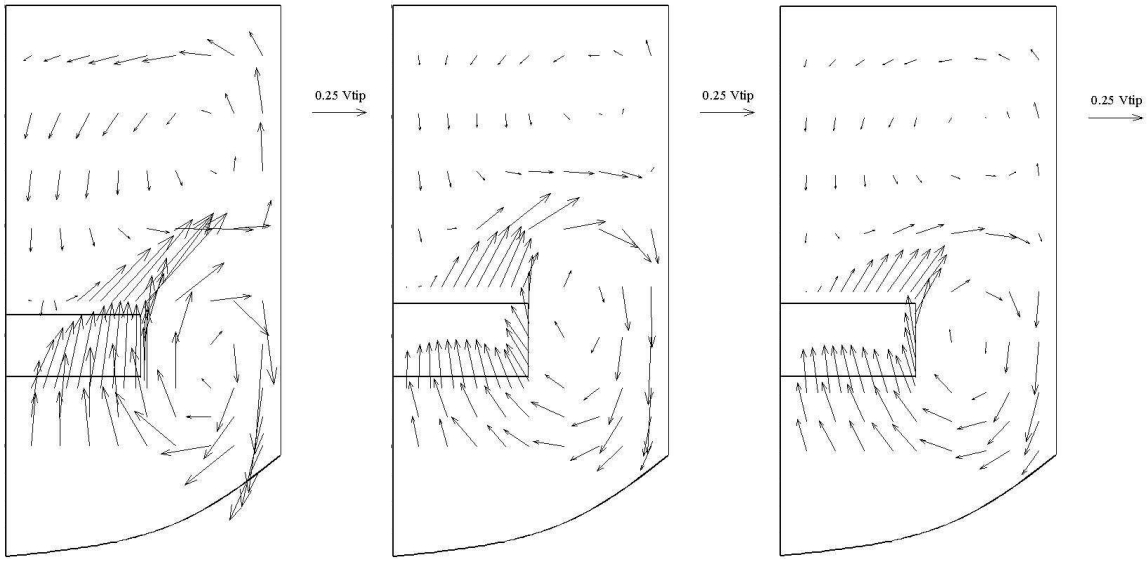

(c) PBT-upwards (d) MTT-upwards (e) MTT-reverse

Figure 2

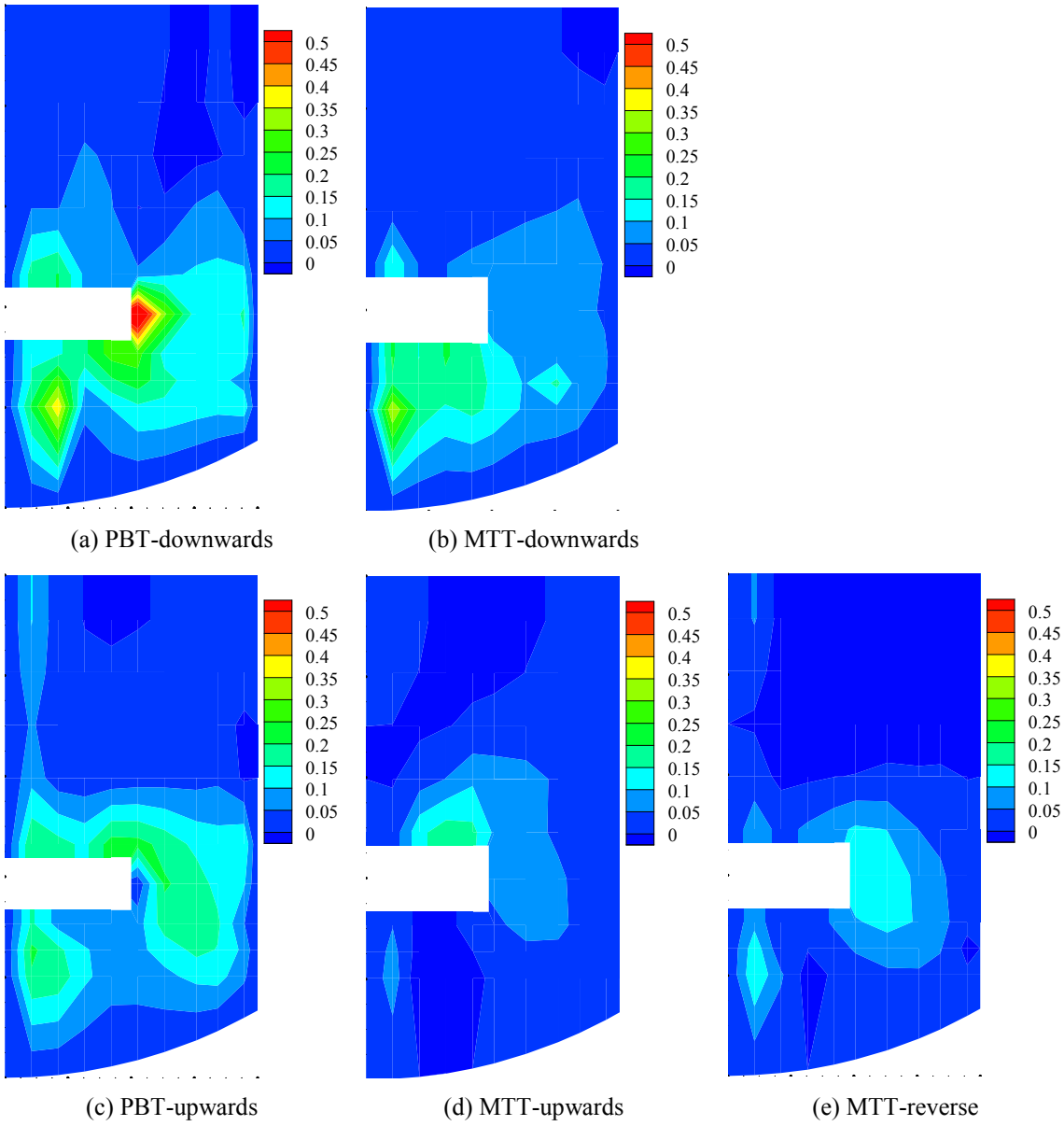

(a) PBT-downwards (b) MTT-downwards

(c) PBT-upwards (d) MTT-upwards (e) MTT-reverse

Figure 3

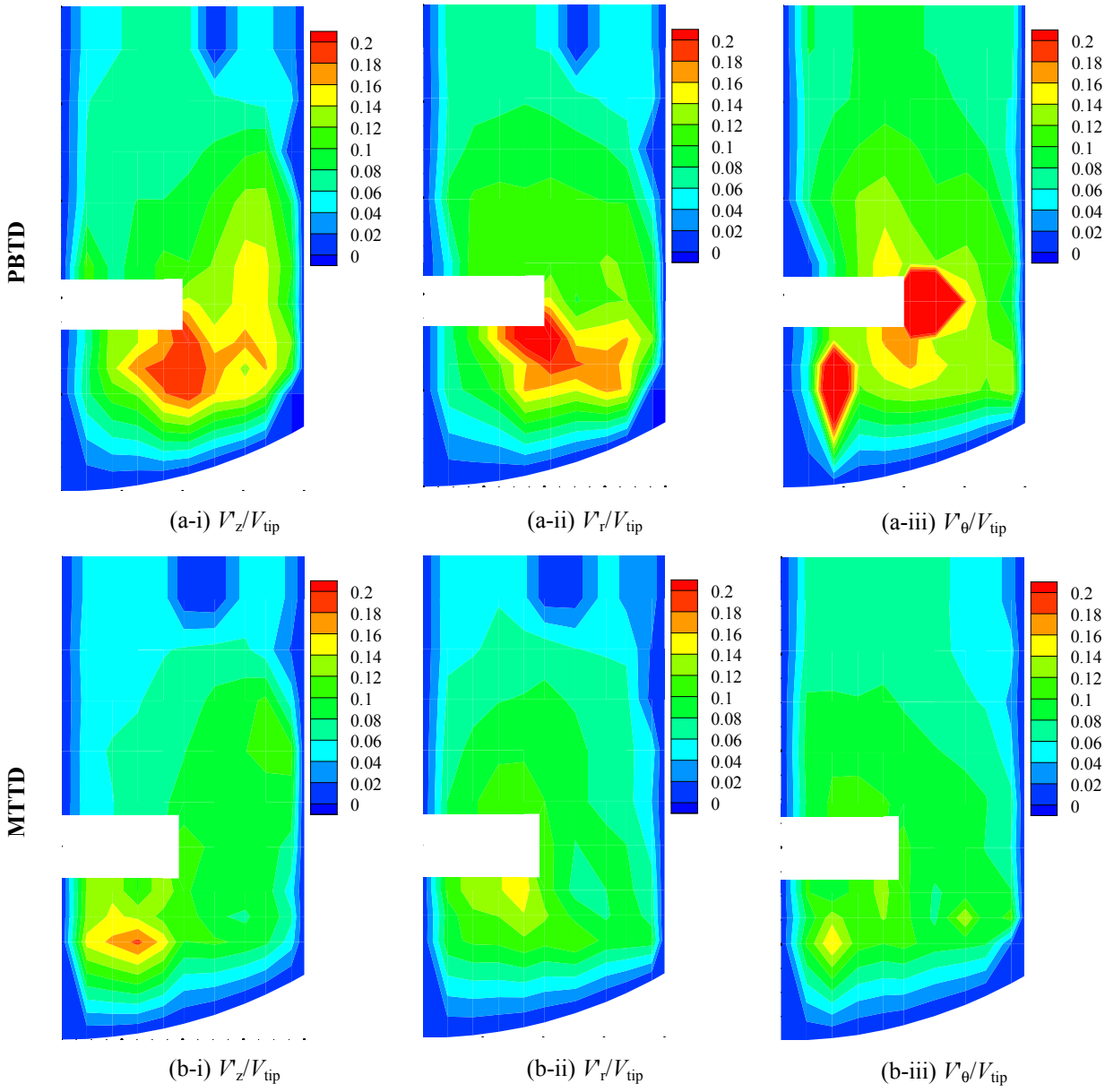
PBTD
MTTD
0.2
0.18
0.16
0.14
0.12
0.1
0.08
0.06
0.04
0.02
0
(a-i) V'_z/V_{tip}
(a-ii) V'_r/V_{tip}
(a-iii) V'_θ/V_{tip}
(b-i) V'_z/V_{tip}
(b-ii) V'_r/V_{tip}
(b-iii) V'_θ/V_{tip}

Figure 4

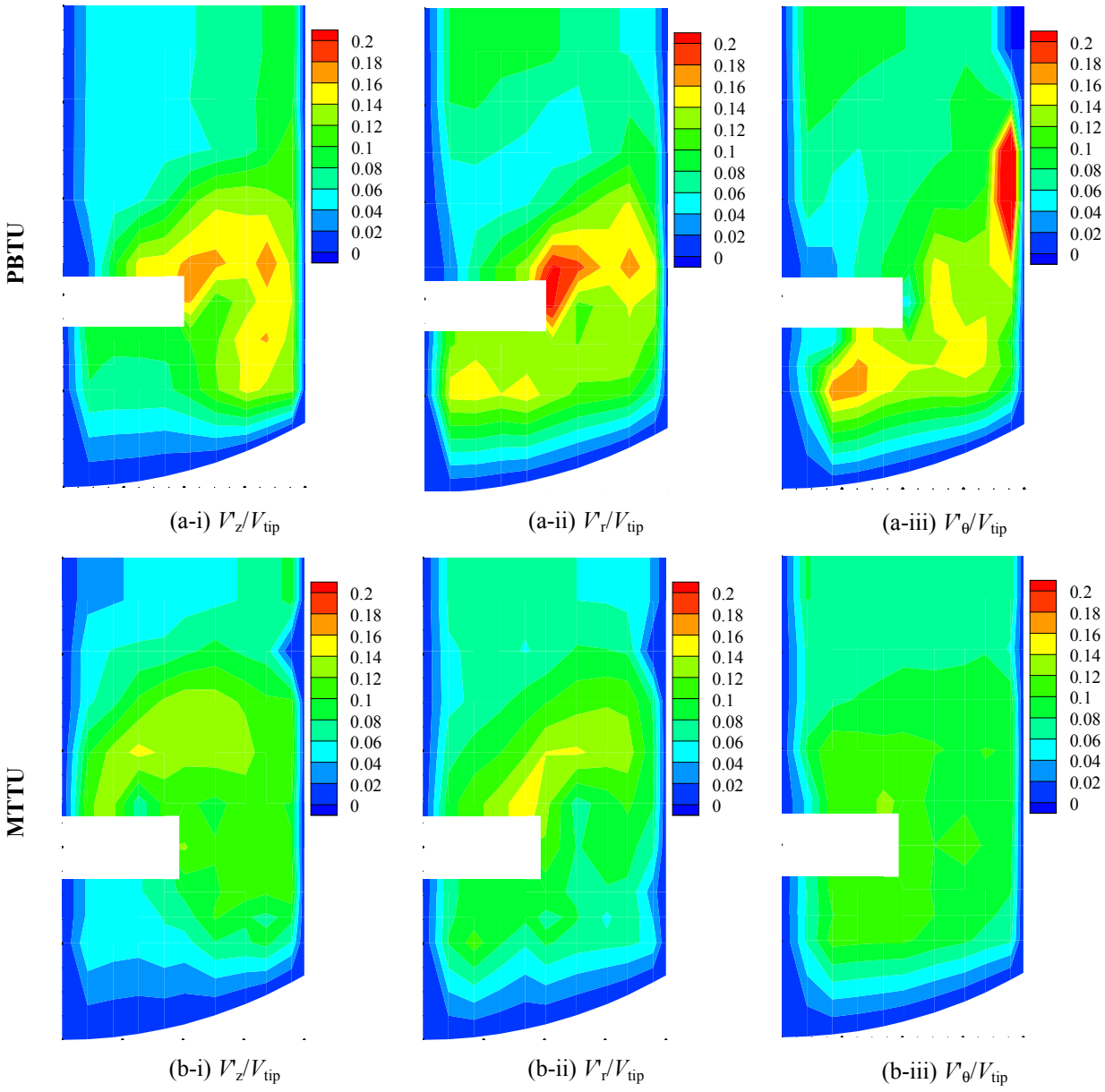
PBTU
MTTU
0.2
0.18
0.16
0.14
0.12
0.1
0.08
0.06
0.04
0.02
0
(a-i) V'_z/V_{tip}
(a-ii) V'_r/V_{tip}
(a-iii) V'_θ/V_{tip}
(b-i) V'_z/V_{tip}
(b-ii) V'_r/V_{tip}
(b-iii) V'_θ/V_{tip}

Figure 5

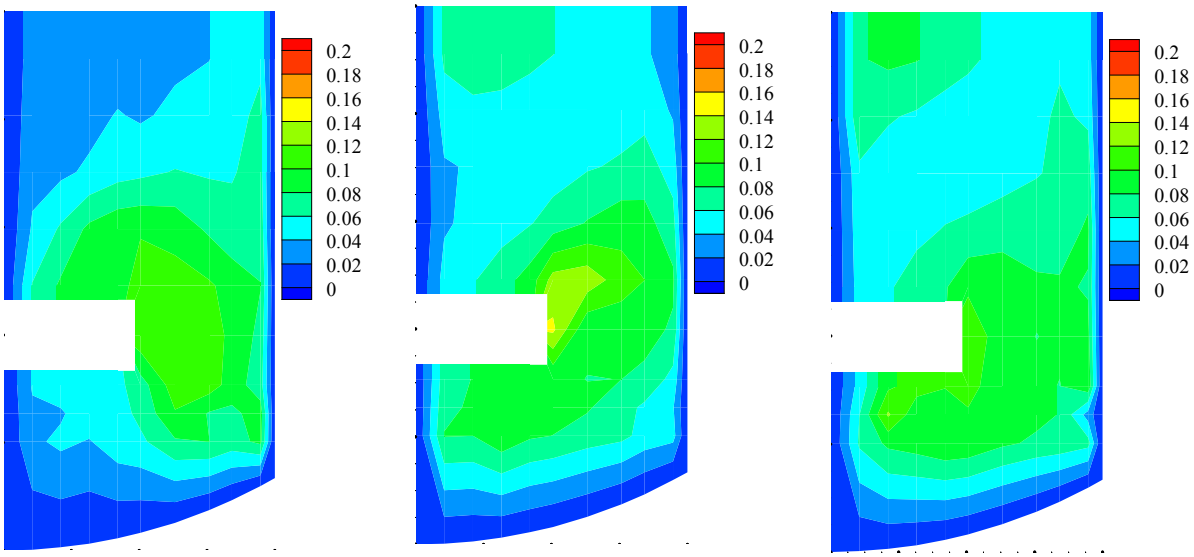

(a-i) V'_z/V_{tip} (a-ii) V'_r/V_{tip} (a-iii) V'_θ/V_{tip}

Figure 6

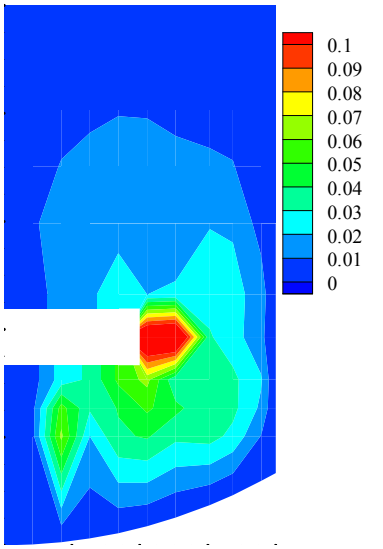

(a) PBTD

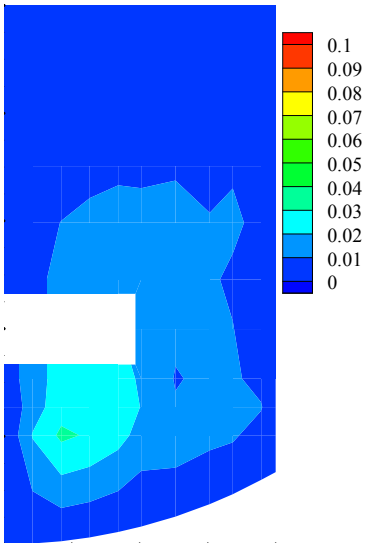

(b) MTTD

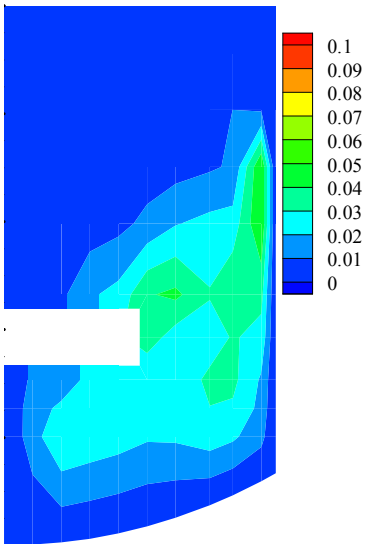

(c) PBTU

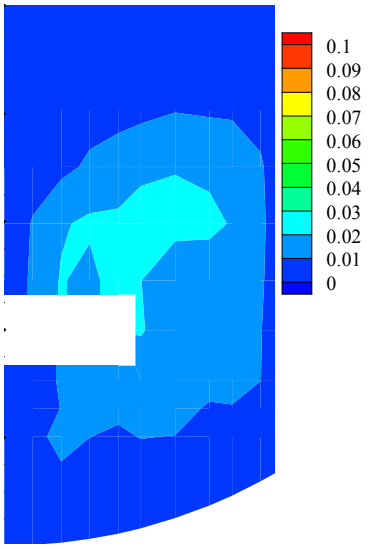

(d) MTTU

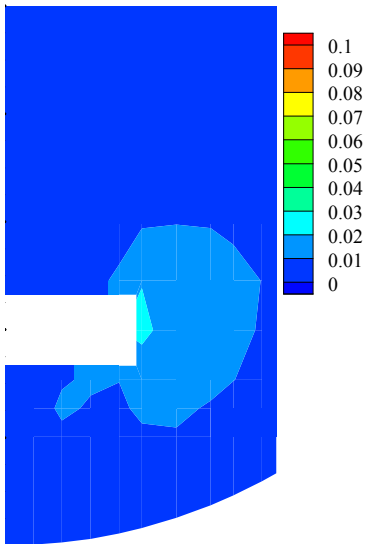

(e) MTTR

Figure 7

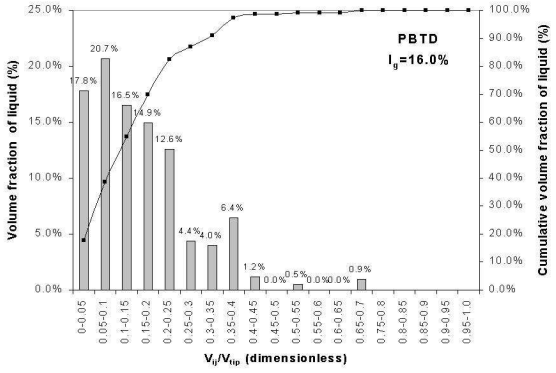

(a) PBTD

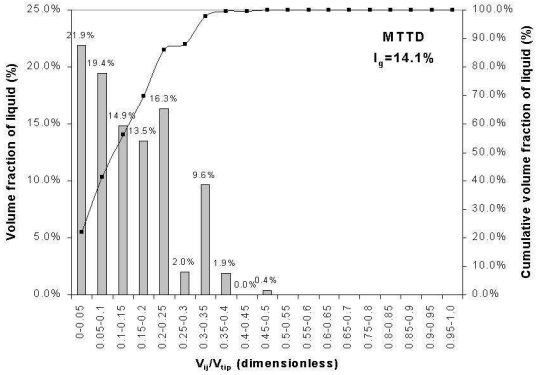

(b) MTTD

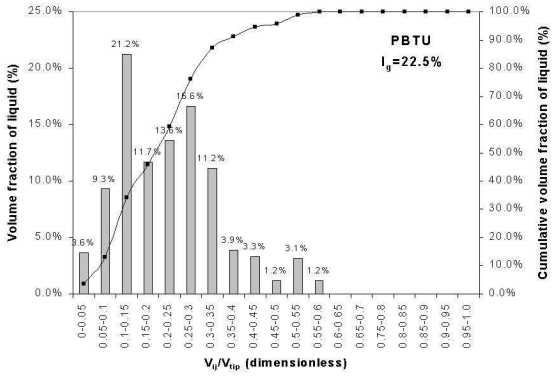

(c) PBTU

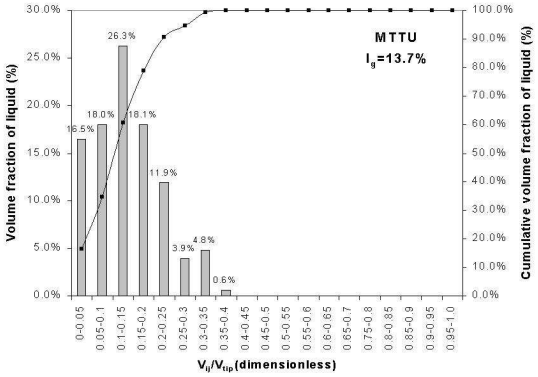

(d) MTTU

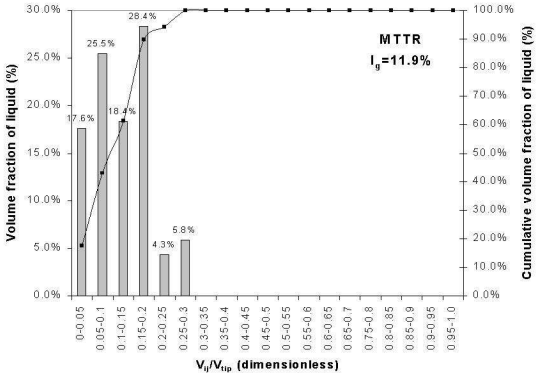

(e) MTTR

Figure 8